How to cite: *Angew. Chem. Int. Ed.* **2023,** *62,* e202217184
International Edition: doi.org/10.1002/anie.202217184
German Edition: doi.org/10.1002/ange.202217184

Organometallic Chemistry

Evidence of Al^{II} Radical Addition to Benzene

Debdeep Mandal, T. Ilgin Demirer, Tetiana Sergeieva, Bernd Morgenstern, Haakon T. A. Wiedemann, Christopher W. M. Kay, and Diego M. Andrada**

Abstract: Electrophilic Al^{III} species have long dominated the aluminum reactivity towards arenes. Recently, nucleophilic low-valent Al^{I} aluminyl anions have showcased oxidative additions towards arenes C–C and/or C–H bonds. Herein, we communicate compelling evidence of an Al^{II} radical addition reaction to the benzene ring. The electron reduction of a ligand stabilized precursor with KC_8 in benzene furnishes a double addition to the benzene ring instead of a C–H bond activation, producing the corresponding cyclohexa-1,3(orl,4)-dienes as Birch-type reduction product. X-ray crystallographic analysis, EPR spectroscopy, and DFT results suggest this reactivity proceeds through a stable Al^{II} radical intermediate, whose stability is a consequence of a rigid scaffold in combination with strong steric protection.

Introduction

The preference of aluminum to adopt its oxidation state Al^{III} has been extensively exploited in the design of trivalent species as Lewis acid catalysts in various organic transformations.[1] In contrast, and despite significant progress in the field, low oxidation states such as Al^{II} and Al^{I} are still considered exotic, and their applications are considerably less numerous.[2] Efforts in this area have been driven by their proven potential to replace transition metals in various catalytic cycles involving bond activation processes.[3]

The first Al^{I} species was reported more than thirty years ago by Schnöckel in the form of a tetrameric species (**I**), which upon thermal conditions, dissociates into its monomeric units.[4] The isolation of the pure monomeric form has been accomplished by increasing the steric demand $AlCp^{R}$ ($Cp^{R} = C_5H_2tBu_3$).[5] Ten years later, the first monomeric neutral Al^{I} compound (**II**) was isolated and characterized by Roesky.[6] The bulky β-diketiminate (NacNac) supporting ligand was the key to providing enough electronic and steric protection to the aluminum center. Over the years, this compound has evolved from a lab curiosity into a valuable reagent, given its ability to participate in various bond activations via oxidative addition.[7] In 2018, the groups of Aldridge and Goicoechea expanded the scope by synthesizing the anionic Al^{I} nucleophilic species, aluminyl anions (**III**), which demonstrate unprecedented reactivity in the oxidative addition on non-polarized C–H and C–C bonds of aromatic hydrocarbons (Scheme 1). Since then, several amido- and alkyl-substituted aluminyl compounds have been prepared and their reactivity has been explored.[8] Recently, examples of neutral mono-coordinated aluminylenes Al^{I} compounds **IV**–**V** have been reported by Liu, Hinz, and Power taking advantage of sterically demanding carbazolyl and terphenyl ligands respectively.[9]

The exotic reactivity of aluminyl anions is currently in the spotlight for the activation of small molecules. Notably, the reaction outcome sharply depends on the nature of the counter cation and its coordination nature with the anionic moiety.[10] The extent of the interaction between the cation and the flanking aryl substituents plays a crucial role in the formation of aluminyl species.[8e,f,11] In this vein, we envisage that bulky silyl groups, instead of aromatic groups, may provide sufficient kinetic stability to isolate Al^{II} radical species, preventing ionic interactions in favor of aluminyl anions. Compared to Al^{I}, dicoordinated Al^{II} radicals are even rarer. This is partially due to the inherent instability of mononuclear neutral Al^{II}/Al^{I} radical species, which prefers to dimerize forming Al–Al single bonded compounds, **VI**–**IX**.[8h,k,12] Thus, a suitable ligand that not only stabilizes the elusive Al^{II} radical but also destabilize dimer form is indispensable for the successful isolation of aluminum radical species. To date, only a few examples **X**–**XI**[13] are known for neutral monomeric aluminum radicals, using cyclic(alkyl)(amino)carbene (CAAC) as stabilization units of the radical centers.

Herein, we report on the unusual *trans* 1,4-addition of two aluminum(II) species to a benzene furnishing a 1,4-

[*] Dr. D. Mandal, T. I. Demirer, Dr. T. Sergeieva, Dr. B. Morgenstern, Dr. D. M. Andrada
General and Inorganic Chemistry Department, University of Saarland
Campus C4.1, 66123 Saarbrücken (Germany)
E-mail: diego.andrada@uni-saarland.de
H. T. A. Wiedemann, Prof. Dr. C. W. M. Kay
Physical Chemistry Department, University of Saarland
Campus B2.2, 66123 Saarbrücken (Germany)
E-mail: christopher.kay@uni-saarland.de
Prof. Dr. C. W. M. Kay
London Centre for Nanotechnology, University College London
17-19 Gordon Street, London WC1H 0AH (UK)

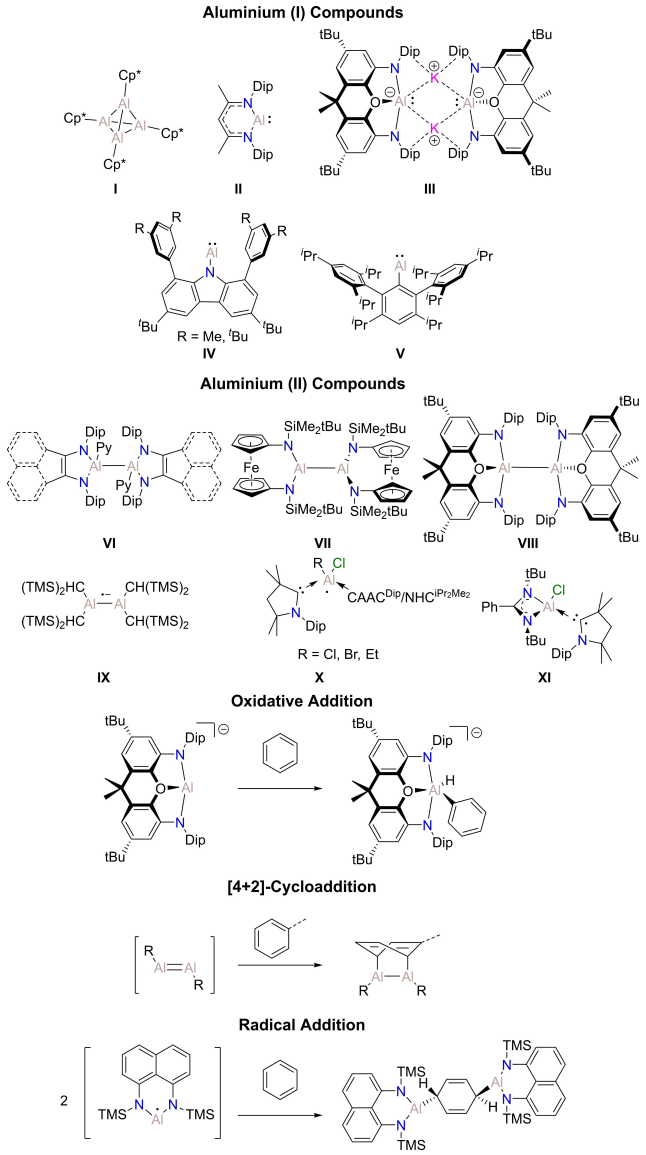

Scheme 1. Selected structures of Al^{I} and Al^{II} compounds. Oxidative addition, [4+2]-cycloaddition, and radical addition. R: Ar* = 2,6-$Dip_2C_6H_3$, Ar** = 2,6-Dip_2-4-TMS-C_6H_2, Bbp = 2,6-[CH-$(TMS)_2]_2C_6H_3$, Tbp = 2,6-[CH-$(TMS)_2]_2$-4-*t*Bu-C_6H_2 [Dip = 2,6-(*i*Pr)$_2C_6H_3$, TMS = Trimethylsilyl].

cyclohexadiene system as a Birch-type reduction reaction product (Scheme 1). The Birch reduction of aromatic compounds is well-established in organic chemistry to produce *cis* and/or *trans* 1,4-disubstituted-cyclohexadienes as hydro, alkyl or silyl derivatives.[14] The groups of Power and Tokitoh have described a *cis* 1,4-addition to toluene and benzene via [4+2]-cycloaddition of a transient dialuminene compound,[15] which has been later stabilized as a dianion[16] or by coordination to Lewis bases.[17] The group of Harder has shown that the combination of the nucleophilic Al^{I} compound (**II**) with the highly Lewis acidic (NacNac)Ca^{+} analogue reduces benzene.[18] Notably, the isolobal Mg compound can also undergo a Birch-type benzene reduction, when the dimerization of the intermediate Mg^{I} radical is prevented by a super bulky spectator ligand ((HC{C(Me)N-[2,6-(3-pentyl)-phenyl]}$_2$)) and a coordinating species, TMEDA (N,N,N′,N′-tetramethylethylenediamine).[19] In the course of the development of this work, the group of Braunschweig reported a similar outcome, in which the aluminum center is coordinated to an *N*-heterocyclic carbene (NHC) and stabilized by a redox-active ferrocenyl substituent.[20] Although it was not possible to isolate or characterize a radical addition to arenes, the authors proposed a plausible radical-based mechanism. We now provide compelling evidence of an in situ generated diamino-substituted Al^{II} radical as a key reactive species for such Birch-type reduction of aromatic molecule.

Results and Discussion

Bis(silylamido)naphthalene derivatives have been recently established as attractive ligands given their unexpectedly high degree of thermodynamic and kinetic stability.[21] This framework provides a characteristic interplay between steric repulsion and dispersive attraction, allowing the isolation of exotic chemical bonds.[22] Thus, the *N*-trimethylsilyl substituted diamino naphthyl amine has been chosen as the supporting ligand for synthesizing the aluminum precursor. Compound **2** was prepared in 67 % yield from a salt metathesis reaction of the respective dilithiated ligand with AlI_3 (Scheme 2a). The molecular structure of compound **2** exhibits a tetra-coordinated aluminum atom located out of the naphthalene plane (Figure 1).[23] The diethylether molecule coordinates to the acidic aluminum center with a bond length of 1.884(4) Å, which is in the range of an Al–O single bond (1.89 Å).[24] This structure is reminiscent to the aluminum iodide stabilized by xanthene ligand (precursor of compound **III**), but the rigid structure carries a longer Al–O bond length (1.967(2) Å).[8a] The Al–N bond lengths are 1.797(5) and 1.803(5) Å, fall in between the typical Al–N single and double bonds (1.97 and 1.73 Å, respectively),[24] indicative of a weak N π-donation. The nitrogen atoms are planar ($\Sigma_4 = 359.5°$), underlining that the location of the aluminum is a consequence of the relatively small bonding pocket of the ligand, i.e. 2.06 Å compared to the xanthene scaffold 4.55 Å in **III**.[25] Note that precursor **III** analogue has longer Al–N bond lengths (1.847(2) Å).[8a]

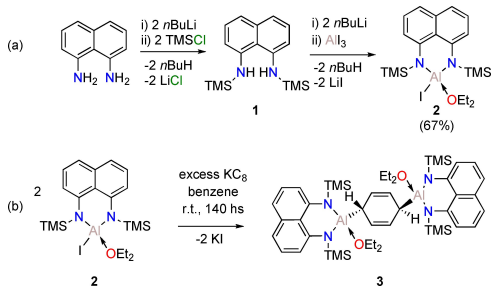

Scheme 2. (a) Synthesis of **1** and **2**. (b) Reduction of **2** with excess of KC_8.

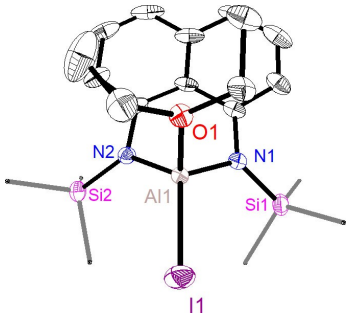

Figure 1. Molecular structure of **2** in the solid state as determined by X-ray crystallography. Thermal ellipsoids set at 50% probability. Hydrogen atoms were omitted for clarity. Selected experimental bond lengths (Å) and bond angles (°): Al1–N1 1.797(5), Al1–N2 1.803(5), Al1–O1 1.884(4), Al1–I1 2.520(2), N1–Si1 1.739(5), N2–Si2 1.742(5), N2–Al1–N1 103.7(2), N1–Al1–I1 118.2(2), N2–Al1–I1 124.0(2).

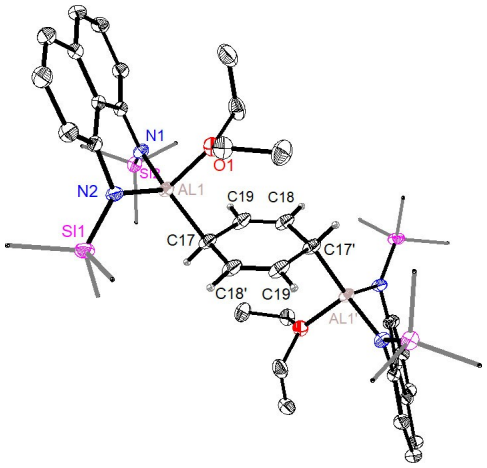

Figure 2. Molecular structure of **3** in the solid state as determined by X-ray crystallography. Thermal ellipsoids set at 50% probability. Nonessential hydrogen atoms were omitted for clarity. Selected experimental and theoretical [TPSSh/def2-SVP] bond lengths (Å) and bond angles (°): Al1–N1 1.8293(8) [1.848], Al1–N2 1.8319(8) [1.850], Al1–O1 1.9151(7) [1.971], Al1–C17 1.9925(9) [2.016], C17–C19 1.503(1) [1.506], C18–C19 1.333(2) [1.349], N1–Al1–N2 101.56(2) [101.7], N1–Al1–C17 121.19(8) [124.4], N1–Al1–C17 124.49(2) [123.0].

In order to prepare the corresponding reduced species (Al^{II} radical or aluminyl Al^{I} anion), we attempted various reducing conditions. The reduction of **2** with conventional reducing agents like metallic Mg, K(mirror), or KC_8 in ethereal solvents (THF, diethyl ether) afforded either an unidentified mixture or decomposition products. Also, reduction of compound **2** with equimolar Jones Mg^{I} reagent or cobaltocene ($Co(Cp)_2$) led to no reaction in benzene solution. While reducing **2** with one equivalent of KC_8 led to incomplete reduction even after several days, stirring a reaction mixture containing compound **2** with an excess of KC_8 (2 equivalents) at room temperature in benzene for 140 hs gave rise to complete conversion (Scheme 2a). The initially expected formation of an aluminyl anion or dialumane species could rapidly be ruled out based on the NMR spectra indicating the occurrence of six new protons symmetrically distributed. In ^{1}H NMR, alongside the expected trimethylsilyl groups ($\delta(^1H) = 0.44$ ppm (s)) and the coordinated diethyl ether ($\delta(^1H) = 3.79$ (sept) and 0.40 ppm(t)), two distinctive singlets at 5.89 (4H) and 2.37 (2H) ppm were observed. In confirmation of the ^{1}H NMR data, the ^{13}C NMR spectrum shows two new signals at chemical shifts of 124.6 and 29.9 ppm. These NMR spectroscopic data compare favorably with the reported quinoid type benzene moiety suggesting a Birch-type reduction product of benzene.[14a,19,20]

After the filtration of the insoluble precipitate from the reaction mixture, an orange solution was obtained. Pale yellow crystals of **3** were grown from concentrated solution after 1 week at 4 °C and the structure was confirmed by X-ray diffraction (Figure 2). As predicted from the ^{1}H NMR chemical shifts, a benzene molecule reacts with two molecules of reduced intermediate of compound **2**, and the resulting molecule **3** exhibits a C_i symmetry. While the tetracoordinated environment around aluminum center from compound **2** is preserved, the bond lengths with the surrounding atoms become longer in **3**, probably because of the steric repulsion with the new C_6H_6 moiety. In this sense, the Al–N bonds to the supporting ligands in **3** (1.8293(8) Å) are longer than in **2**. Also, the coordinating ether molecule has a 1.9151(7) Å bond length, while the distortion degree ($\Sigma_4 = 347°$) supports a weak interaction ($D_e = 29.1$ and 25.6 kcal mol^{-1} for **2** and **3**, respectively). The bond lengths between the aluminum atom and the carbon atom of the benzene (1.9925(9) Å) in **3** are slightly shorter than the expected Al–C single bond (2.01 Å),[24] and also than those reported for the Birch reduction by Brand et al. 2.060(3)/2.073(3) Å,[18] by Dhara et al. 2.064(3)/2.059(3) Å,[20] and also from the products resulting from the [4+2]-cycloaddition, i.e. 2.000(2)/2.003(2) Å,[15a] and 2.028(5)/2.020(5) Å.[15b] As in the case of compound **2**, the Al atom in **3** remains out of the plane of the ligand. Notably, the C18–C19 bond length of 1.333(2) Å is comparable to the double bond (1.34 Å), while the C17–C19 bond length of 1.503(1) indicates a C–C single bond (1.50 Å).

The new adduct **3** is indefinitely stable at ambient temperature in the solid state under argon atmosphere. Notably, the addition of the aluminum units to the benzene ring in the 1,4 fashion leading to the quinoid type of structure through de-aromatization benzene can only be explained by the presence of an *in situ* generated Al^{II} radical species.[14b] We explored the reaction paths using density functional theory (DFT) at the PCM(benzene)-TPSSh/def2-TZVPP//TPSSh/def2-SVP level of theory (see Supporting Information for further details). Figure 3 shows the computed reaction profiles along with some key optimized structures. The reaction starts with one electron reduction of compound **2**, with the elimination of iodine in the form of KI to generate a new radical species **INT1**, where the ether molecule is coordinated. The corresponding radical anion of **2** is computed as an unstable species which is prone to the elimination of iodine ($\Delta G = -11.4$ kcal mol^{-1}). The strength of the bond between Al and O in **INT1** is significantly reduced, and its release is endergonic by 2.6 kcal mol^{-1},

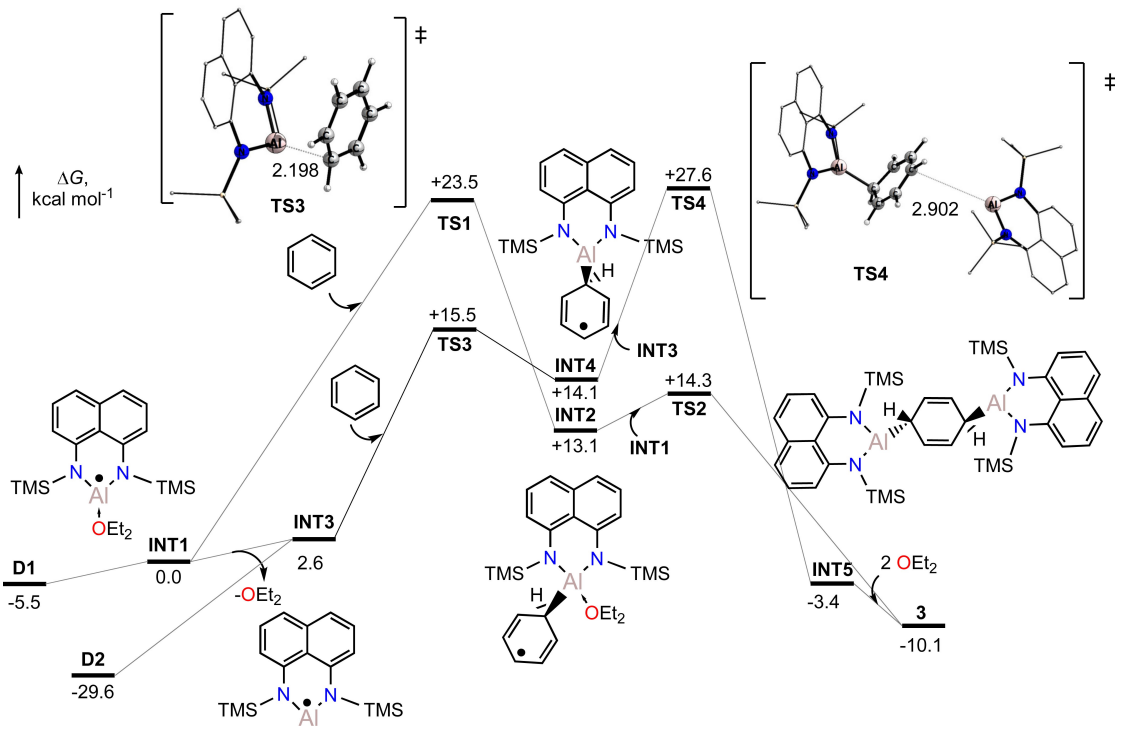

Figure 3. Gibbs free energy (ΔG in kcal mol^{-1}) profile at the PCM(benzene)-TPSSh/def2-TZVPP//TPSSh/def2-SVP level of theory for the reduction of **2** in benzene solvent. Transition state structures are shown, where nonessential hydrogens were omitted for clarity.

forming the radical species **INT3**. Despite not being experimentally isolated, both **INT1** and **INT3** can dimerize to form their respective dialumane **D1** and **D2** since the process is exergonic by 5.5 and 29.6 kcal mol^{-1}, respectively. The monomer and dimer species can exist in equilibrium.[26] Nonetheless, the probability of meeting a benzene solvent molecule is higher than meeting another **INT1** or **INT3** to dimerize, similar to the situation of a heterobimetallic Ca/Al Birch-reduction.[18] Thus, the radical addition to a molecule of benzene is the first step of the reaction. While the most stable radical species **INT1** requires 23.5 kcal mol^{-1}, the corresponding addition from **INT3** has lower energy barrier 15.5 kcal mol^{-1}. The energy needed to form the intermediate **INT2** and **INT4** is 13.1 and 14.1 kcal mol^{-1}, respectively. The formed intermediates are thermodynamically unfavored, and they can easily collapse back to **INT1** or **INT3**, as the difference in energy to **TS3** is very small. However, in a high-pressure regime where molecular collisions are efficient enough to cool the otherwise rovibrationally hot intermediates, causing it to be in thermal equilibrium with the environment. To produce the observed product **3**, a second **INT1** or **INT3** must meet **INT2** or **INT4**. The second step of the reaction course is computed to be fast when the ether molecule is coordinated **TS3**, while the **INT4** and **INT3** react via **TS4** with a Gibbs energy of 27.6 kcal mol^{-1} relative to the reactants. The overall thermodynamics of the reaction is favorable by 10.1 kcal mol^{-1}. Potentially, different isomers are possible according to the position and geometry of the second radical addition. Our calculations suggest the observed *trans*- structure in **3** as the most stable isomer (see Figure S32).

The optimized structure for **3** is in good agreement with the crystal structure (Figure 2). The calculated NPA charge of +2.14 (Al) is in line with previously assigned of Al^{III}.[18] The total charge on the $C_6H_6^{2-}$ fragment (−1.37 e) is in agreement with its strongly reduced nature. While the C atoms directly attached to the Al atoms bear a (C17 = −0.89 e), the vinylic C atoms has only (C18/C19 = −0.22 e). The chemical bond Al–C is rather ionic (Figure S33 and Table S5) with a Wiberg bond order of 0.41 au.

It is noteworthy that the experimental conditions and the computational calculations agree on a rather slow reduction process under the given conditions. The rate-determining step is computed as the first step consisting of the radical addition of aluminum species to the benzene molecule with an energy of 15.5 kcal mol^{-1}, and a second step with 13.5 kcal mol^{-1}. Therefore, this result predicts the presence of relatively stable radical species **INT1–4** in solution. In order to prove the radical addition reaction, we recorded the time dependence of the reduction of **2** with continuous wave (cw) EPR spectroscopy at X-band frequencies. For that, dry C_6H_6 was added to the solid mixture of compound **2** and KC_8 (1:2.2 ratio) at room temperature under inert conditions. An aliquot of reaction mixture (supernatant solution) was transferred into a quartz EPR tube at various time intervals. The aliquot was then diluted with dry C_6H_6, and the EPR spectra were measured. This procedure was repeated over several days. Figure 4a shows

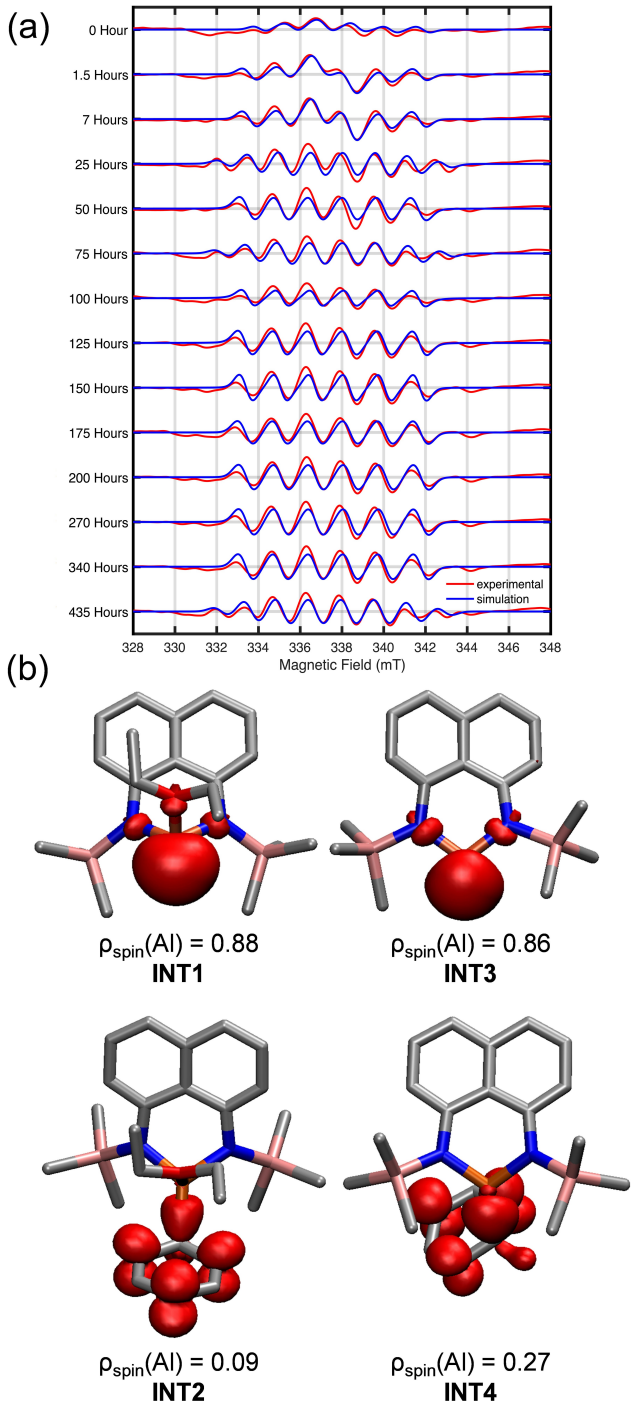

Figure 4. (a) EPR spectra of (1 : 2) reduction reaction between compound **2** and KC_8 at various time intervals. Simulation parameters: $g_{iso} = 2.0057$, $A_{iso}(^{27}Al) = 1.63$ mT. (b) Spin density (isovalue 0.004 a.u.) and Mulliken spin-density plots of **INT1–4**. H atoms have been omitted for clarity.

the experimentally obtained EPR spectra together with their simulations.

All EPR spectra are dominated by the sextet that results from the coupling of the unpaired electron with the aluminum center (^{27}Al, 100 % natural abundance, $I = 5/2$). At early times, our simulations suggest the presence of two species with g_{iso} of 2.0057 and 2.0051 and isotropic hyperfine couplings (*hfc*), $A_{iso}(^{27}Al)$ of 1.63 mT and 1.54 mT, respectively. However, on a longer times scale, the EPR radical formation corresponds mainly to one species (g_{iso} of 2.0057 and $A_{iso}(^{27}Al)$ of 1.63 mT). Note that after 50 hours of reaction a third 11 lines species is detected with g_{iso} of 2.00638 and $A_{iso}(^{27}Al)$ of 1.30/1.26 mT. The magnitude of the *hfc*s in this species is larger than those reported for metal-base spin aluminum radicals such as $[R_2AlAlR_2]^{\bullet-}$ (1.11 mT),[27] and carbene-stabilized aluminum radicals (0.93–1.25 mT).[13a,c] In contrast, aluminum radical complexes with ligand-based spin have smaller $A(^{27}Al)$ values (0.13–0.46 mT).[28] The *hfcs* of Al centered radicals strongly depend on the *s*-orbital character via pyramidalization.[29] For instance, the radical anion $[AlH_3]^{\bullet-}$ displays an isotropic *hfc* of 15.4 mT with a deviation from planarity of $\Sigma_4 = 331.8°$, while the $[Al(SiMetBu_2)_3]^{\bullet-}$ which is more planar $\Sigma_4 = 358.4°$ exhibits a *hfc* of 6.2 mT.[30] Furthermore, the resulting cyclohexadienyl radical adduct from the $[AlH_3]^{\bullet-}$ addition to benzene affords an $A_{iso}(^{27}Al)$ of 5.4 mT.[29] The stronger participation of the *s*-orbital character has also been suggested as responsible for the higher *hfcs* of $[R_2AlAlR]^{\bullet}$ ($A_{iso}(^{27}Al)$ of 2.18 and 1.89 mT), compared to the aforementioned $[R_2AlAlR_2]^{\bullet-}$.[31] Figure 4b shows the calculated spin density of the main radical species **INT1–4**. In general, the calculations indicate the presence of an unpaired electron mainly located at the aluminum atom, with a small contribution of the nitrogen atoms of the supporting ligand (Table S7). EPR calculations provided an estimated *hfc* of 36.6 mT and 41.8 mT for **INT1** and **INT3**, respectively, in line with the strong *s*-orbital character of the unpaired electron. On the other hand, the **INT2** and **INT4** display a smaller *hfc*, namely 7.7 mT and 8.8 mT, respectively. Note, that the predicted *hfcs* depend on a rather flat potential energy surface. We have also considered the dialanes $\mathbf{D1}^{\bullet-}$ and $\mathbf{D2}^{\bullet-}$ radical anion species (Table S7). The calculations suggest g_{iso} of 2.00212 and $A_{iso}(^{27}Al)$ of –0.10 mT for $\mathbf{D1}^{\bullet-}$ and g_{iso} of 2.00174 and $A_{iso}(^{27}Al)$ of 10.1/9.8 mT $\mathbf{D2}^{\bullet-}$. The EPR signal consisting of 11 lines is probably due to $\mathbf{D2}^{\bullet-}$, which under the reaction conditions dissociates ($\Delta G = -28.0\ kcal\,mol^{-1}$) to give **INT3**. However, given the mismatch between the experimental and theoretical *hfc* values, the EPR cannot be unambiguously assigned.

The manipulation of adduct **3** in different solvents indicated that the ether molecule can be easily exchanged. Therefore, we envisioned the use of stronger σ-donors such NHC or CAAC for stabilizing the radical species and re-aromatizing the benzene molecule. However, the reaction process led only to a ligand exchange with 1,3-di*iso*propyl-4,5-dimethylimidazol-2-ylidene ($NHC^{iPr2Me2}$), while $CAAC^{Dip}$ shows no reaction (Scheme 3).

Furthermore, all our attempts to isolate the radical species or activate different aromatic compounds such as toluene, xylene and biphenyl with the in situ generated Al^{II} radical were unsuccessful. In contrast to former benzene reductions,[15b,18] leaving a C_6D_6 solution of compounds **3**, **4**, or **5** at room temperature does not lead to any detectable decrease of the NMR signals corresponding to the C_6H_6 moiety. This observation holds even after heating for 24 hrs

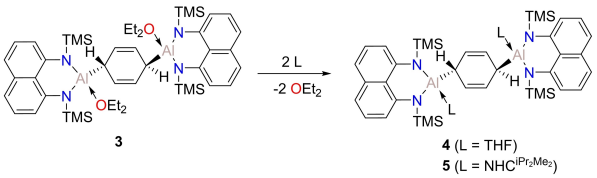

Scheme 3. Ligand exchange reaction of **3**.

at 60 °C, thus indicating the intermolecular exchange of the C_6H_6 molecule is not possible.

The low reactivity of the intermediates is advantageous for the EPR detection, but the lifetime measurements by other spectroscopic methods like UV/Vis are precluded by the absorption of **2**. Additionally, due to the reaction setup, TEMPO cannot be used as radical scavenger. Instead, to trap or examine the transient radical, we conducted the reduction of **2** with KC_8 in the presence of 1 equiv of $CAAC^{Dip}$ in benzene at room temperature, which afforded a deep yellow solution (Scheme 4). The related product is NMR silent, and unfortunately, despite numerous crystallization attempts no crystals could be obtained. Nonetheless, the formation of **6** was confirmed by Fourier-transform ion cyclotron resonance-mass spectrometry showing a peak at m/z 613.38 $[LAl(cAAC)]^+$ (Figure S25). Although the ether molecule could bind to the Al center, our calculations suggest a very weak coordination energy (D_e = 11.6 kcal mol^{-1}).

We were also able to monitor the progress of this reaction via EPR spectroscopy. In this case, the EPR spectra show a broad four-line asymmetric signal shape (Figure 5a). The simulations suggest the occurrence of two species. At short reaction time (1.5 hrs), a radical with g = 2.0033(2) and $A(^{14}N)$ = 0.48 mT is the major radical species, probably the $CAAC^{Dip}$ radical anion. A minor component increases with time, with g = 2.0026(3) and $A_{iso}(^{27}Al)$ = 0.47 mT. Our theoretical calculations suggest a *hfc* of **6** of $A_{iso}(^{27}Al)$ = 0.34 mT (Figure 5b). This result is in good agreement with previous ligand-base radical of aluminum **XI** with a experimental $A_{iso}(^{27}Al)$ = 0.93 mT.[13c]

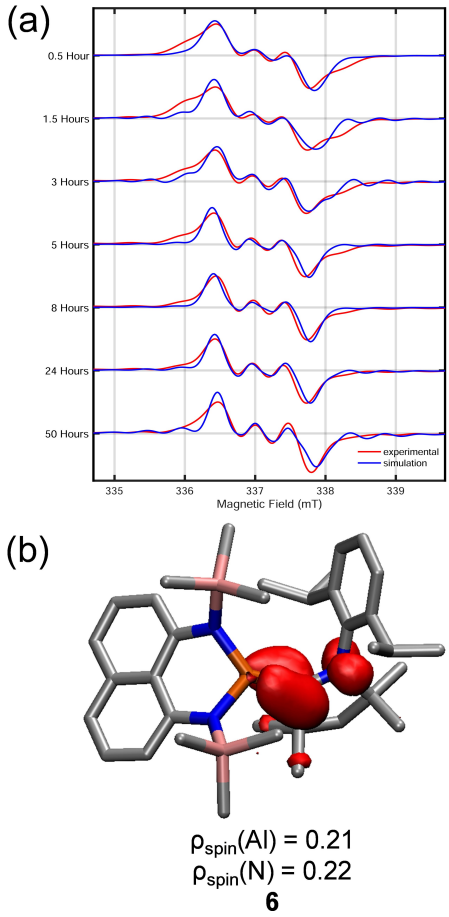

Figure 5. (a) EPR spectra of (1 : 2) reduction reaction of compound **2** with KC_8 in the presence of $CAAC^{Dip}$ at various time intervals. Simulation parameters, **6**: g_{iso} = 2.0026(3) (2.00261), $A_{iso}(^{27}Al)$ = = 0.47 mT (0.34 mT), $A_{iso}(^{14}N)$ = 0.48 mT (0.62 mT); $[CAAC^{Dip}]^{\bullet-}$: g_{iso} = 2.0033(2), $A_{iso}(^{14}N)$ = 0.48 mT, $A_{iso}(^{1}H)$ = 0.21 mT. (b) Spin density (isovalue 0.003 a.u.) and Mulliken spin-density plots of **6**. H atoms have been omitted for clarity.

Conclusion

In conclusion, we have described a new reaction mode of aluminum(II) species. In great contrast to the well-known Al^{III} and Al^{I} reactions towards arenes, the designed aluminum complex produces a stable radical intermediate upon reduction, leading to a Birch reduction type reaction. This result is a consequence of the rigid scaffold of the supporting ligand in combination with silyl protecting groups. Thus, the absence of protecting aromatic substituent on the neighboring nitrogen atoms probably prevents the formation of an ionic pair between a putative aluminyl anion and counter cations, leaving room for an aluminum radical. Current efforts are directed at the isolation and further spectroscopic characterization of the aluminum radical.

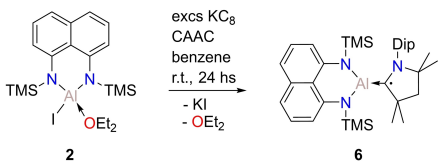

Scheme 4. Reduction of **2** with excess of KC_8 in the presence of $CAAC^{Dip}$.

Acknowledgements

The work at University of Saarland has been supported by the ERC StG (EU805113). DM thanks the Alexander von Humboldt Foundation for the postdoctoral fellowship. DMA thanks Prof. Dr. Scheschkewitz for his kind support. All authors gratefully acknowledge the suggestions from M.Sc. S. Danés, M.Sc. E. Sabater, Dr. H.-G. Korth, and Prof. Dr. Simon Aldridge. Instrumentation and technical

assistance for this work were provided by the Service Center Mass Spectrometry and the Service Center X-ray Diffraction, with financial support from Saarland University and the German Science Foundation (project number INST 256/506-1). EPR spectroscopy was performed on spectrometers purchased with support of the State of Saarland and the German Science Foundation (project number INST 256/535-1) Open Access funding enabled and organized by Projekt DEAL.

The authors declare no conflict of interest.Data Availability Statement

The data that support the findings of this study are available in the supplementary material of this article.

Conflict of Interest

The authors declare no conflict of interest.

Keywords: Aluminum · EPR Spectroscopy · Low-Valent Compounds · Radicals · Structure Elucidation

[1] a) T. Krahl, E. Kemnitz, *Catal. Sci. Technol.* **2017**, *7*, 773–796; b) T. Krahl, E. Kemnitz, *J. Fluorine Chem.* **2006**, *127*, 663–678; c) S. Saito, in *Main Group Metals in Organic Synthesis*, Wiley-VCH, Weinheim, **2004**, pp. 189–306; d) G. A. Olah, V. P. Reddy, G. K. S. Prakash, in *Kirk-Othmer Encyclopedia of Chemical Technology*, Wiley, Hoboken, **2000**; e) V. P. Reddy, G. K. S. Prakash, in *Kirk-Othmer Encyclopedia of Chemical Technology*, Wiley, Hoboken, **2000**, pp. 1–49.

[2] a) P. P. Power, *Nature* **2010**, *463*, 171–177; b) M. Melaimi, R. Jazzar, M. Soleilhavoup, G. Bertrand, *Angew. Chem. Int. Ed.* **2017**, *56*, 10046–10068; *Angew. Chem.* **2017**, *129*, 10180–10203; c) R. L. Melen, *Science* **2019**, *363*, 479–484; d) Y. Su, R. Kinjo, *Chem. Soc. Rev.* **2019**, *48*, 3613–3659; e) C. Weetman, S. Inoue, *ChemCatChem* **2018**, *10*, 4213–4228; f) P. Bellotti, M. Koy, M. N. Hopkinson, F. Glorius, *Nat. Chem. Rev.* **2021**, *5*, 711–725.

[3] a) C. Weetman, H. Xu, S. Inoue, in *Encyclopedia of Inorganic and Bioinorganic Chemistry*, Wiley, Hoboken, **2011**, pp. 1–20; b) K. Hobson, C. J. Carmalt, C. Bakewell, *Chem. Sci.* **2020**, *11*, 6942–6956.

[4] a) C. Dohmeier, C. Robl, M. Tacke, H. Schnockel, *Angew. Chem. Int. Ed. Engl.* **1991**, *30*, 564–565; *Angew. Chem.* **1991**, *103*, 594–595; b) H. Sitzmann, M. F. Lappert, C. Dohmeier, C. Üffing, H. Schnöckel, *J. Organomet. Chem.* **1998**, *561*, 203–208.

[5] A. Hofmann, T. Tröster, T. Kupfer, H. Braunschweig, *Chem. Sci.* **2019**, *10*, 3421–3428.

[6] C. Cui, H. W. Roesky, H.-G. Schmidt, M. Noltemeyer, H. Hao, F. Cimpoesu, *Angew. Chem. Int. Ed.* **2000**, *39*, 4274–4276; *Angew. Chem.* **2000**, *112*, 4444–4446.

[7] Y. Liu, J. Li, X. Ma, Z. Yang, H. W. Roesky, *Coord. Chem. Rev.* **2018**, *374*, 387–415.

[8] a) J. Hicks, P. Vasko, J. M. Goicoechea, S. Aldridge, *Nature* **2018**, *557*, 92–95; b) M. M. D. Roy, J. Hicks, P. Vasko, A. Heilmann, A.-M. Baston, J. M. Goicoechea, S. Aldridge, *Angew. Chem. Int. Ed.* **2021**, *60*, 22301–22306; *Angew. Chem.* **2021**, *133*, 22475–22480; c) R. J. Schwamm, M. D. Anker, M. Lein, M. P. Coles, *Angew. Chem. Int. Ed.* **2019**, *58*, 1489–1493; *Angew. Chem.* **2019**, *131*, 1503–1507; d) R. J. Schwamm, M. P. Coles, M. S. Hill, M. F. Mahon, C. L. McMullin, N. A. Rajabi, A. S. S. Wilson, *Angew. Chem. Int. Ed.* **2020**, *59*, 3928–3932; *Angew. Chem.* **2020**, *132*, 3956–3960; e) M. J. Evans, M. D. Anker, M. G. Gardiner, C. L. McMullin, M. P. Coles, *Inorg. Chem.* **2021**, *60*, 18423–18431; f) T. X. Gentner, M. J. Evans, A. R. Kennedy, S. E. Neale, C. L. McMullin, M. P. Coles, R. E. Mulvey, *Chem. Commun.* **2022**, *58*, 1390–1393; g) S. Kurumada, S. Takamori, M. Yamashita, *Nat. Chem.* **2020**, *12*, 36–39; h) K. Koshino, R. Kinjo, *J. Am. Chem. Soc.* **2020**, *142*, 9057–9062; i) S. Grams, J. Eyselein, J. Langer, C. Färber, S. Harder, *Angew. Chem. Int. Ed.* **2020**, *59*, 15982–15986; *Angew. Chem.* **2020**, *132*, 16116–16120; j) S. Kurumada, K. Sugita, R. Nakano, M. Yamashita, *Angew. Chem. Int. Ed.* **2020**, *59*, 20381–20384; *Angew. Chem.* **2020**, *132*, 20561–20564; k) I. L. Fedushkin, M. V. Moskalev, A. N. Lukoyanov, A. N. Tishkina, E. V. Baranov, G. A. Abakumov, *Chem. Eur. J.* **2012**, *18*, 11264–11276.

[9] a) J. D. Queen, A. Lehmann, J. C. Fettinger, H. M. Tuononen, P. P. Power, *J. Am. Chem. Soc.* **2020**, *142*, 20554–20559; b) X. Zhang, L. L. Liu, *Angew. Chem. Int. Ed.* **2021**, *60*, 27062–27069; *Angew. Chem.* **2021**, *133*, 27268–27275; c) A. Hinz, M. P. Muller, *Chem. Commun.* **2021**, *57*, 12532–12535.

[10] a) J. Hicks, P. Vasko, J. M. Goicoechea, S. Aldridge, *J. Am. Chem. Soc.* **2019**, *141*, 11000–11003; b) J. Hicks, P. Vasko, J. M. Goicoechea, S. Aldridge, *Angew. Chem. Int. Ed.* **2021**, *60*, 1702–1713; *Angew. Chem.* **2021**, *133*, 1726–1737; c) J. Hicks, P. Vasko, A. Heilmann, J. M. Goicoechea, S. Aldridge, *Angew. Chem. Int. Ed.* **2020**, *59*, 20376–20380; *Angew. Chem.* **2020**, *132*, 20556–20560.

[11] S. Grams, J. Mai, J. Langer, S. Harder, *Dalton Trans.* **2022**, *51*, 12476–12483.

[12] a) P. Henke, T. Pankewitz, W. Klopper, F. Breher, H. Schnöckel, *Angew. Chem. Int. Ed.* **2009**, *48*, 8141–8145; *Angew. Chem.* **2009**, *121*, 8285–8290; b) V. A. Dodonov, W. Chen, L. Liu, V. G. Sokolov, E. V. Baranov, A. A. Skatova, Y. Zhao, B. Wu, X.-J. Yang, I. L. Fedushkin, *Inorg. Chem.* **2021**, *60*, 14602–14612; c) Y. Zhao, Y. Liu, L. Yang, J.-G. Yu, S. Li, B. Wu, X.-J. Yang, *Chem. Eur. J.* **2012**, *18*, 6022–6030; d) W. Uhl, *Z. Naturforsch. B* **1988**, *43*, 1113–1118.

[13] a) B. Li, S. Kundu, A. C. Stückl, H. Zhu, H. Keil, R. Herbst-Irmer, D. Stalke, B. Schwederski, W. Kaim, D. M. Andrada, G. Frenking, H. W. Roesky, *Angew. Chem. Int. Ed.* **2017**, *56*, 397–400; *Angew. Chem.* **2017**, *129*, 407–411; b) S. Kundu, S. Sinhababu, S. Dutta, T. Mondal, D. Koley, B. Dittrich, B. Schwederski, W. Kaim, A. C. Stückl, H. W. Roesky, *Chem. Commun.* **2017**, *53*, 10516–10519; c) M. M. Siddiqui, S. Banerjee, S. Bose, S. K. Sarkar, S. K. Gupta, J. Kretsch, N. Graw, R. Herbst-Irmer, D. Stalke, S. Dutta, D. Koley, H. W. Roesky, *Inorg. Chem.* **2020**, *59*, 11253–11258; d) B. Li, B. L. Geoghegan, H. M. Weinert, C. Wolper, G. E. Cutsail, S. Schulz, *Chem. Commun.* **2022**, *58*, 4372–4375.

[14] a) P. W. Rabideau, Z. Marcinow, The Birch Reduction of Aromatic Compounds. In *Organic Reactions*, **2004**, pp. 1–334, https://doi.org/10.1002/0471264180.or042.01; b) H. E. Zimmerman, *Acc. Chem. Res.* **2012**, *45*, 164–170.

[15] a) R. J. Wright, A. D. Phillips, P. P. Power, *J. Am. Chem. Soc.* **2003**, *125*, 10784–10785; b) T. Agou, K. Nagata, N. Tokitoh, *Angew. Chem. Int. Ed.* **2013**, *52*, 10818–10821; *Angew. Chem.* **2013**, *125*, 11018–11021.

[16] R. J. Wright, M. Brynda, P. P. Power, *Angew. Chem. Int. Ed.* **2006**, *45*, 5953–5956; *Angew. Chem.* **2006**, *118*, 6099–6102.

[17] a) P. Bag, A. Porzelt, P. J. Altmann, S. Inoue, *J. Am. Chem. Soc.* **2017**, *139*, 14384–14387; b) C. Weetman, A. Porzelt, P. Bag, F. Hanusch, S. Inoue, *Chem. Sci.* **2020**, *11*, 4817–4827.

[18] S. Brand, H. Elsen, J. Langer, W. A. Donaubauer, F. Hampel, S. Harder, *Angew. Chem. Int. Ed.* **2018**, *57*, 14169–14173; *Angew. Chem.* **2018**, *130*, 14365–14369.
[19] T. X. Gentner, B. Rösch, G. Ballmann, J. Langer, H. Elsen, S. Harder, *Angew. Chem. Int. Ed.* **2019**, *58*, 607–611; *Angew. Chem.* **2019**, *131*, 617–621.
[20] D. Dhara, F. Fantuzzi, M. Härterich, R. D. Dewhurst, I. Krummenacher, M. Arrowsmith, C. Pranckevicius, H. Braunschweig, *Chem. Sci.* **2022**, *13*, 9693–9700.
[21] N. J. Roberts, E. R. Johnson, S. S. Chitnis, *Organometallics* **2022**, *41*, 2180–2187.
[22] a) K. M. Marczenko, J. A. Zurakowski, K. L. Bamford, J. W. M. MacMillan, S. S. Chitnis, *Angew. Chem. Int. Ed.* **2019**, *58*, 18096–18101; *Angew. Chem.* **2019**, *131*, 18264–18269; b) K. M. Marczenko, S. S. Chitnis, *Chem. Commun.* **2020**, *56*, 8015–8018; c) A. Koner, T. Sergeieva, B. Morgenstern, D. M. Andrada, *Inorg. Chem.* **2021**, *60*, 14202–14211.
[23] Deposition numbers 2193647 (for 2), 2193648 (for 3), 2193649 (for 4), and 2193650 (for 5) contain the supplementary crystallographic data for this paper. These data are provided free of charge by the joint Cambridge Crystallographic Data Centre and Fachinformationszentrum Karlsruhe Access Structures service.
[24] P. Pyykko, *J. Chem. Phys. A* **2015**, *119*, 2326–2337.
[25] P. Federmann, T. Bosse, S. Wolff, B. Cula, C. Herwig, C. Limberg, *Chem. Commun.* **2022**, *58*, 13451–13454.
[26] a) P. P. Power, *Chem. Rev.* **2003**, *103*, 789–810; b) J. Moilanen, P. P. Power, H. M. Tuononen, *Inorg. Chem.* **2010**, *49*, 10992–11000.
[27] W. Uhl, A. Vester, W. Kaim, J. Poppe, *J. Organomet. Chem.* **1993**, *454*, 9–13.
[28] W. Kaim, *J. Am. Chem. Soc.* **1984**, *106*, 1712–1716.
[29] J. R. M. Giles, B. P. Roberts, *J. Chem. Soc. Chem. Commun.* **1981**, 1167–1168.
[30] M. Nakamoto, T. Yamasaki, A. Sekiguchi, *J. Am. Chem. Soc.* **2005**, *127*, 6954–6955.
[31] N. Wiberg, T. Blank, W. Kaim, B. Schwederski, G. Linti, *Eur. J. Inorg. Chem.* **2000**, 1475–1481.

Manuscript received: November 22, 2022
Accepted manuscript online: January 3, 2023
Version of record online: February 17, 2023